

## SUPPLEMENTARY INFORMATION

# Doubly Crosslinked Poly(vinyl amine) microgels: Hydrogels of Covalently Inter-linked Cationic Microgel Particles

Sineenat Thaiboonrod, Amir H. Milani and Brian R. Saunders\*

*Biomaterials Research Group, Manchester Materials Science Centre, School of Materials,  
The University of Manchester, Grosvenor Street, Manchester, M1 7HS, U.K.*

### Microgel compositions

The compositions of SX PNVF, SX PVAM and SX PVAM-GMA microgels were determined from the ratio of the %N/%C values ( $R_{NC}$ ) measured from elemental analysis (See Table S1).

**Table S1.** Elemental analysis data for the microgels.

Code	%C	%H	%N	$R_{NC}^a$
SX PNVF	48.60	7.80	17.10	0.352
SX PVAM	40.35	9.03	19.03	0.472
SX PVAM-GMA	43.86	8.76	15.39	0.351
DX PVAM	42.61	8.64	14.93	0.350

<sup>a</sup>  $R_{NC} = \%N/\%C$ . The errors for these values are  $\pm 0.001$ .

### SX PNVF microgel composition

The following equation was established from the general composition of SX PNVF, i.e., PNVF<sub>1-x</sub>-NVE<sub>x</sub> (Scheme 1(a)) and was used to determine the value for mole fraction of NVE incorporated,  $x$ .

$$x = \frac{1.1662 - 3R_{NC}}{7R_{NC} - 1.1662} \quad (\text{S1})$$

Equation (S1) was derived using the structure for PNVF-NVE shown in Scheme 1(a). The value for  $x$  was calculated as 0.09. The composition was PNVF<sub>0.91</sub>-NVE<sub>0.09</sub>. This matched the stoichiometric ratios of NVF and NVE used during preparation.

### SX PVAM composition

The extent of hydrolysis of SX PNVF to SX PVAM microgel was calculated using elemental analysis data for SX PVAM (Table S1) and the general formula shown for SX PVAM in Scheme 1(a). It was assumed that the ratio of VAM to BEV units was the same as that for NVF to NVEE prior to hydrolysis (Scheme 1(a)). The equation used to calculate the extent of hydrolysis ( $= 100 y$ ) was:

$$y = \frac{3.595R_{NC} - 1.2653}{1.085R_{NC}} \quad (\text{S2})$$

Equation (S2) was derived using the structure for PNVF-NVE shown in Scheme 1(a) and the general formula,  $[\text{PVAM}_{0.91}\text{-BEV}_{0.09}]_y\text{-}[\text{PNVF}_{0.91}\text{-NVE}_{0.09}]_{1-y}$ . The value for  $y$  was calculated to be 0.84.

### **SX PVAM-GMA composition**

The following equation was used to determine the extent of GMA functionalisation ( $z$ ) for SX PVAM-GMA (Scheme 1(a)).

$$z = \frac{0.2344}{R_{NC}} - 0.497 \quad (\text{S3})$$

Equation (S3) was derived using the structure shown in Scheme 1(a) for SX PVAM-GMA and the values determined above for  $x$  and  $y$ , i.e.,  $[(\text{PVAM}_{1-z}\text{-(VAM-GMA)}_z)_{0.91}\text{-BEVAME}_{0.09}]_{0.84}\text{-}[\text{PNVF}_{0.91}\text{-NVE}_{0.09}]_{0.16}$ . The calculated value for  $z$  was 0.17. That value equates to an overall GMA mole fraction of  $(0.17 \times 0.91 \times 0.84 =) 0.13$ .

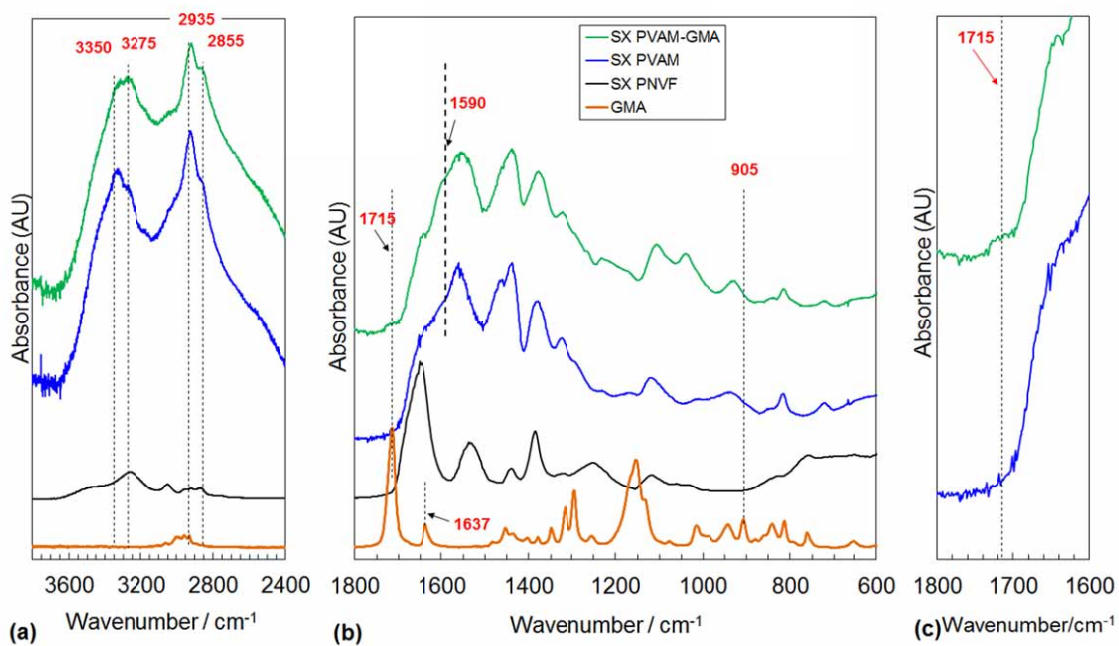


**Fig. S1. FTIR spectra for various microgels.** A spectrum for GMA is shown for comparison.

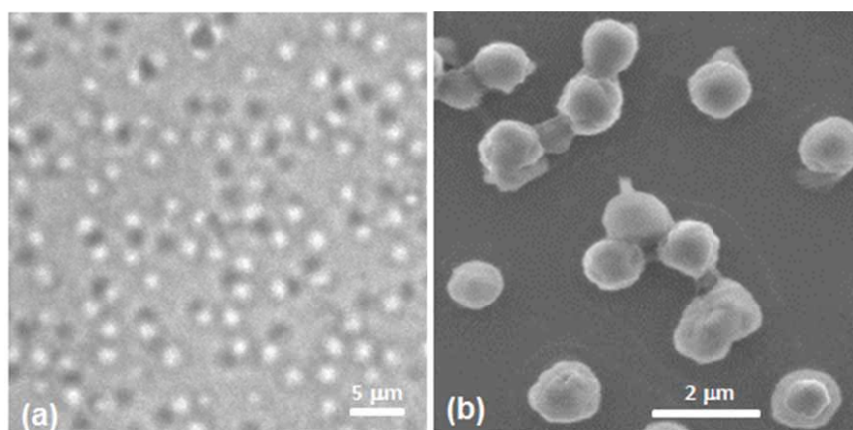


**Fig. S2. Optical microscopy (a) and SEM (b) images for SX PVAM particles.** The microgel particles were dispersed in water at pH = 7 for (a) and were deposited from aqueous dispersion at pH = 9 for (b).

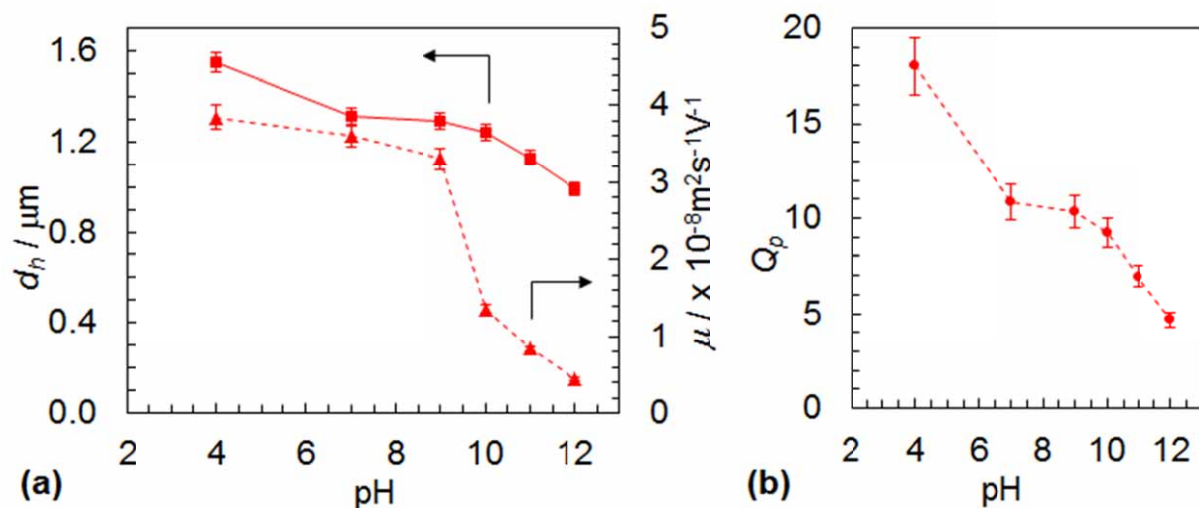


**Fig. S3. pH-dependent properties for SX PVAM microgel particles.** (a) shows the variations of the hydrodynamic diameter and electrophoretic mobility with pH. (b) shows the pH-dependence of the particle swelling ratio (see text).

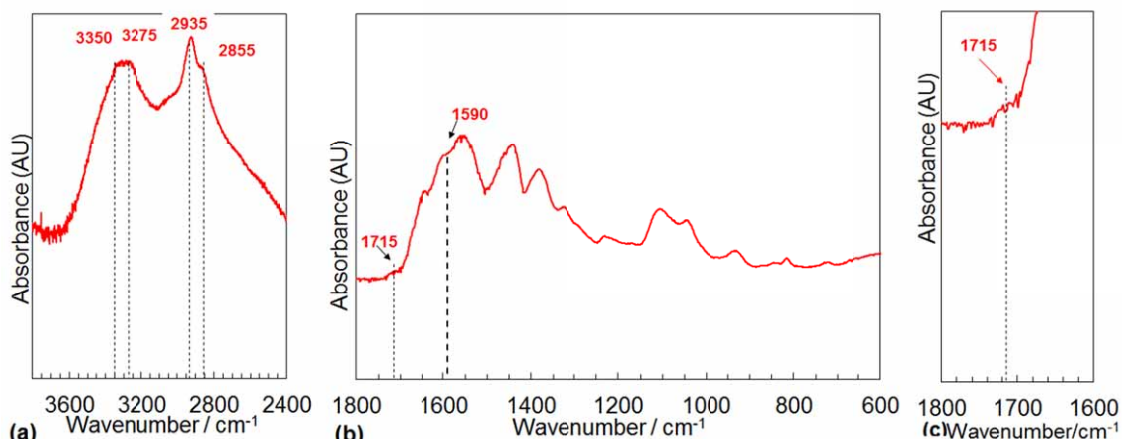


**Fig. S4. FTIR spectra for DX PVAM microgel.**

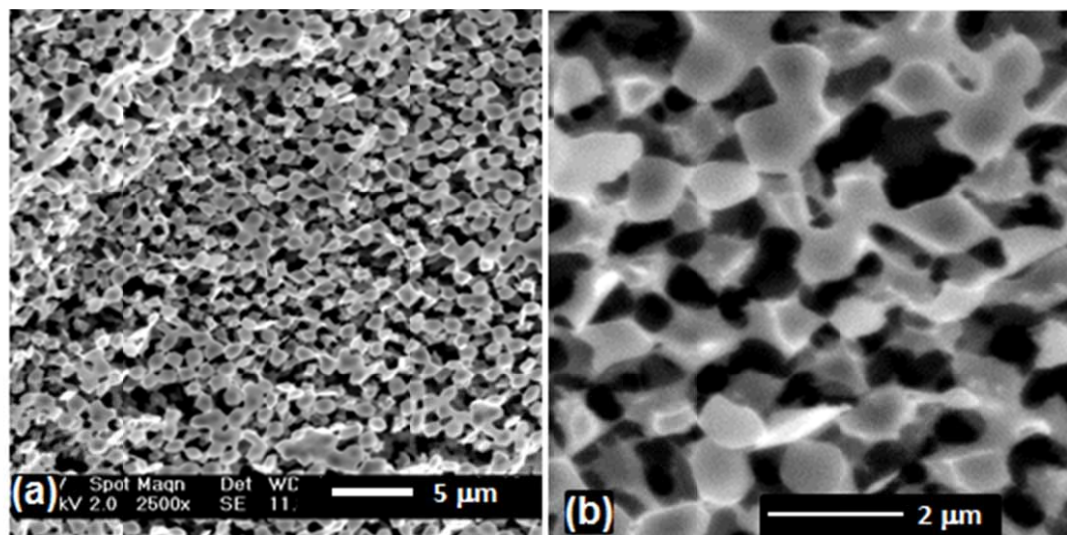


**Fig. S5. SEM images for freeze-dried SX PVAM-GMA ( $\phi_{hs} = 0.10$ ).**

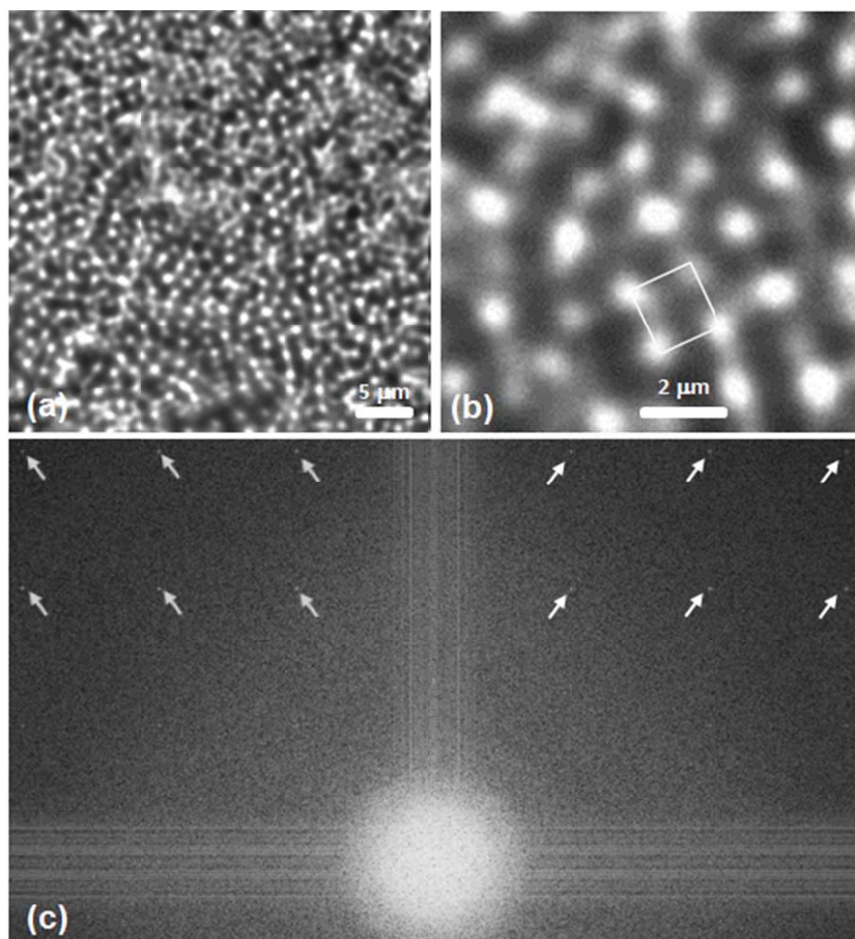


**Fig. S6. Morphologies of SX PVAM gels in the hydrated state.** Optical micrographs for SX PVAM ((a) and (b)) gels. (c) shows an FFT image from (a). The arrows indicate highlight some of the bright points present ( $\phi_{hs} = 0.10$ ).

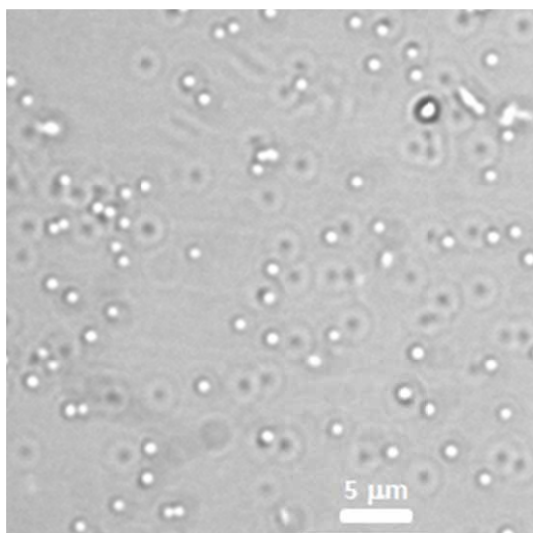


**Fig. S7.** Optical micrograph of PNVF particles dispersed in ethanol.



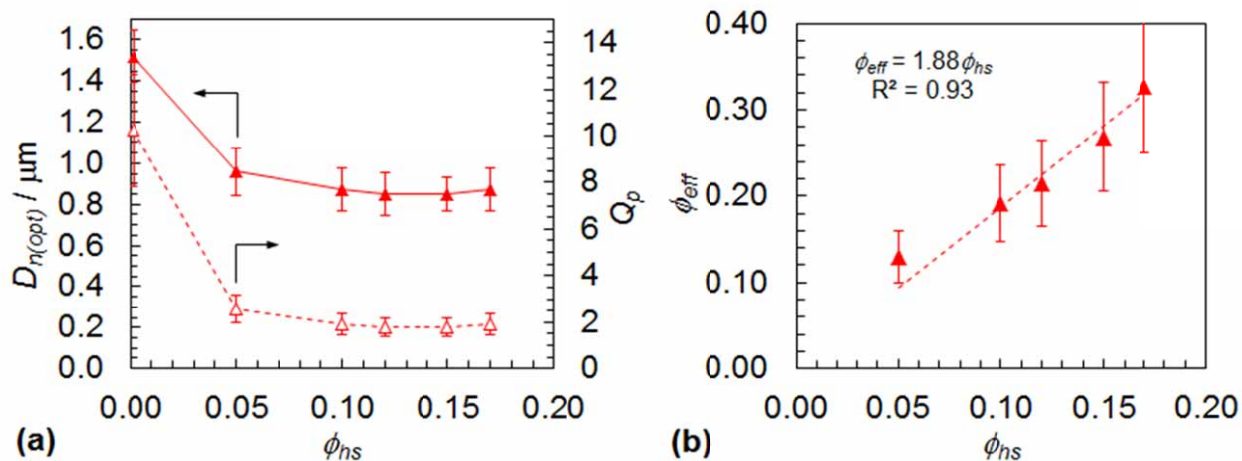


**Fig. S8. Particle size and swelling dependences on polymer volume fraction for SX PVAM gels.** (a) shows the variation of the particle size and particle volume fraction with microgel concentration. (b) shows the calculated variation of the effective polymer volume fraction with microgel concentration.

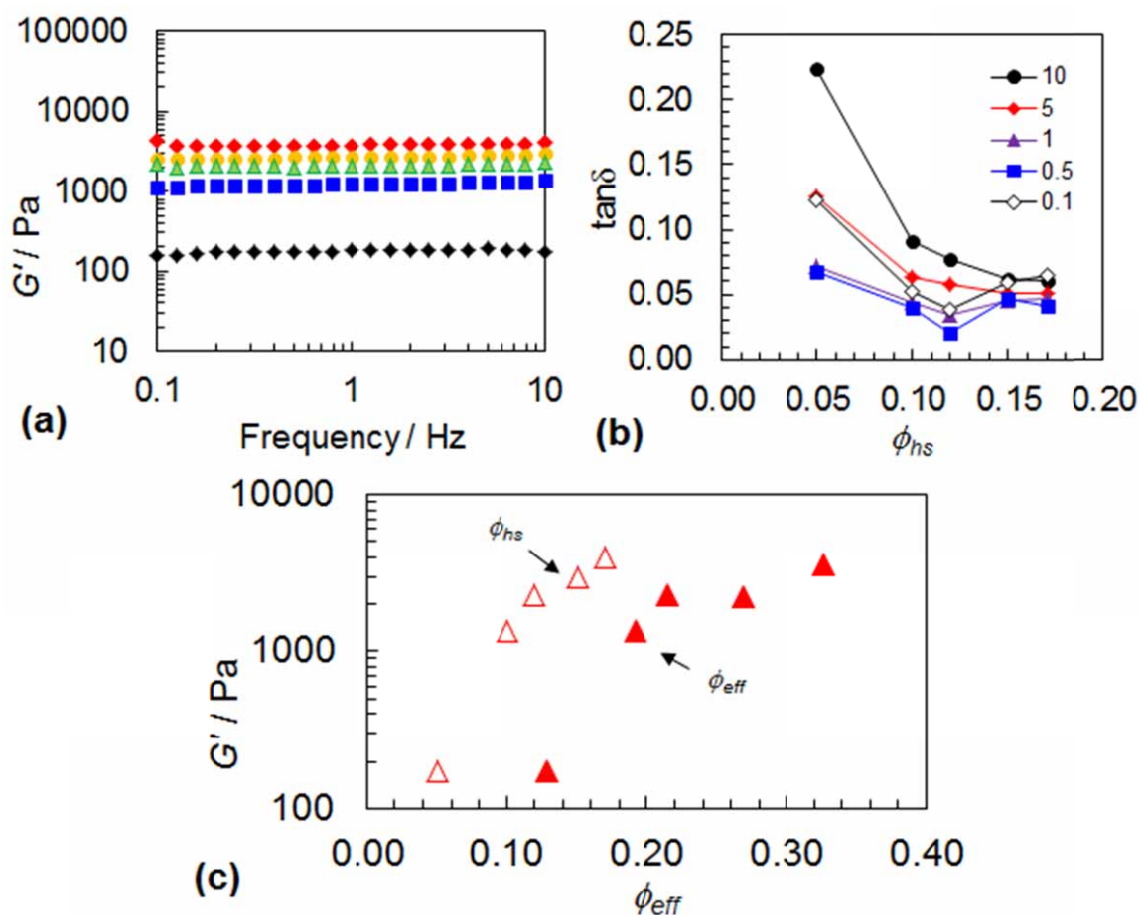


**Fig. S9. SX PVAM frequency sweep data.** (a) shows the frequency dependence for  $G'$ . (b) shows the variation of  $\tan \delta$  with  $\phi_{hs}$  at different frequencies which are shown in the legend in Hz. (c) shows the variation of  $G'$  with  $\phi_{hs}$  and  $\phi_{eff}$  plotted in semi-logarithmic form.

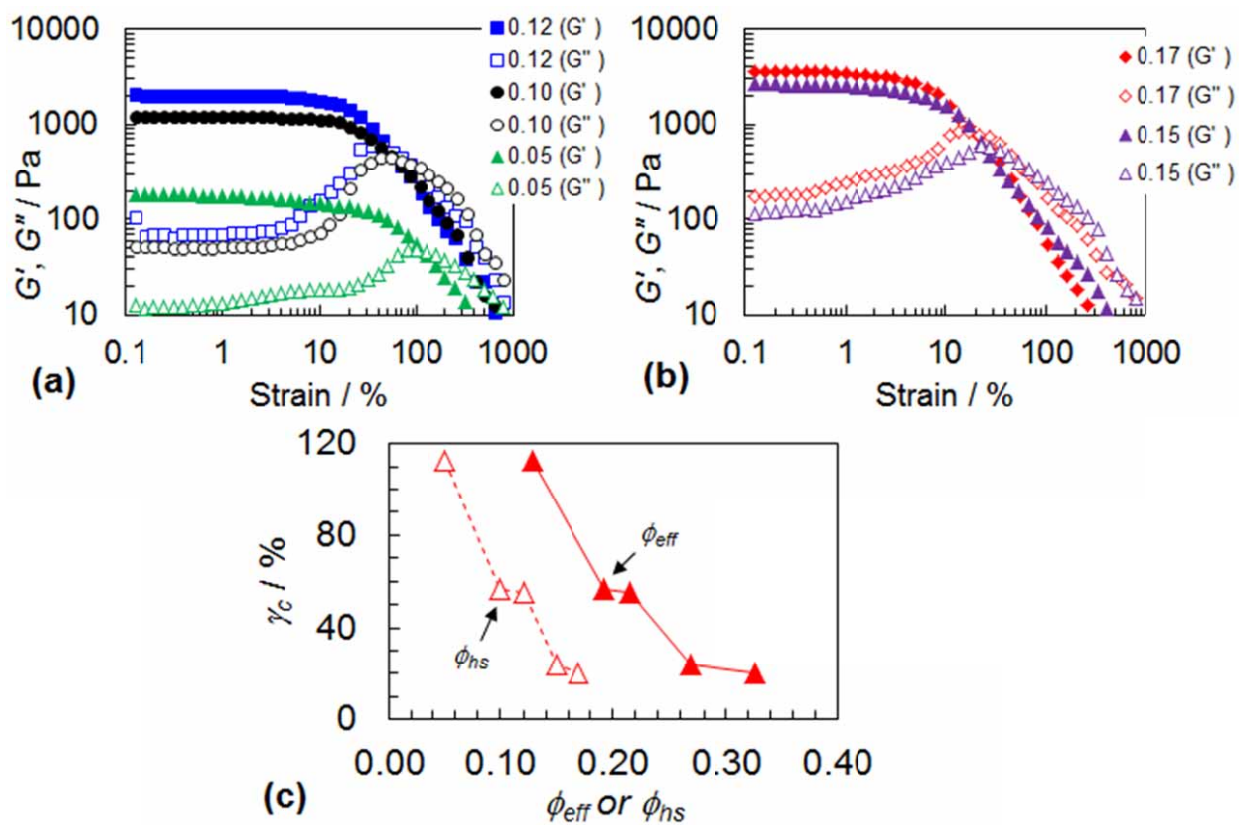


**Fig. S10. SX PVAM strain-sweep data.** (a) and (b) show the variation of  $G'$  and  $G''$  with strain at different  $\phi_{hs}$  values (legend). (c) shows the variation of the yield strain  $\gamma_c$  with  $\phi_{hs}$  and  $\phi_{eff}$